Journal of Power Sources 248 (2014) 1127–1132

Contents lists available at ScienceDirect

Journal of Power Sources

journal homepage: www.elsevier.com/locate/jpowsour

Organically functionalized titanium oxide/Nafion composite proton exchange membranes for fuel cells applications

Dafne Cozzi [a], Catia de Bonis [a], Alessandra D'Epifanio [a,*], Barbara Mecheri [a], Ana C. Tavares [b], Silvia Licoccia [a]

[a] Department of Chemical Science and Technologies, University of Rome "Tor Vergata", Via della Ricerca Scientifica, 00133 Rome, Italy
[b] Institut National de la Recherche Scientifique, Énergie Matériaux Télécommunications (INRS-EMT), 1650 Boulevard Lionel Boulet, Varennes, QC J3X 1S2, Canada

HIGHLIGHTS

- Organically-modified ceramic material (TiO_2–RSO_3H) with high proton conductivity.
- Composite based Nafion membrane electrolyte working at T 140 °C.
- Reduced methanol permeability.

ARTICLE INFO

Article history:
Received 12 April 2013
Received in revised form
13 September 2013
Accepted 10 October 2013
Available online 25 October 2013

Keywords:
Organically functionalized ceramic powder
Proton exchange membrane
Proton conductivity
Direct methanol fuel cells

ABSTRACT

An organically-modified ceramic material (TiO_2–RSO_3H) to be used as filler in Nafion-based composite membranes was synthesized by covalently grafting propylsulfonic acid groups on the surface of TiO_2 nanoparticles.

Higher ion exchange capacity (IEC) and proton conductivity of the hybrid material (one order of magnitude higher for the functionalized filler) reflected in superior performance of Nafion/TiO_2–RSO_3H composite membranes compared to Nafion. The highest conductivity value was obtained for the composite membrane containing 10 wt. % TiO_2–RSO_3H (σ = 0.08 S cm^{-1} at 140 °C). The membranes were tested in a DMFC single cell. The presence of the filler resulted in a general enhancement in the cell response, in terms of both higher power density (PD) delivered and lower methanol crossover with respect to unfilled Nafion membrane. The DMFC containing N_10TiO_2–RSO_3H membrane showed the best performance at 110 °C with a PD of 64 mW cm^{-2}, corresponding to a PD improvement of about 40% with respect to that of Nafion membrane.

1. Introduction

The main advantages of Direct Methanol Fuel Cells (DMFCs) with respect to hydrogen-operating FCs are the higher energy density of the fuel, the low cost of methanol which can be produced from many sources such as natural gas, coal and biomass, and the ease of transportation of the liquid fuel which could be supplied to the public using the existing infrastructure [1]. However, the fuel crossover through the electrolyte from the anode to the cathode and the slow oxidation kinetics of methanol lower the power density and efficiency of DMFCs. Strategies to improve DMFCs performance include operation at high temperature to increase the reactions rate and the tolerance of the anode electrocatalyst to CO, as well as the use of an electrolyte membrane with reduced methanol permeability [2].

Nafion is the most widely used perfluorinated sulphonic acid electrolyte for both hydrogen and methanol-fed proton exchange membrane fuel cells due to its high proton conductivity and chemical and mechanical stability [3]. Nevertheless, Nafion membranes show a strong dependence of proton conductivity on the membrane hydration level and a high crossover rate of methanol [4]. Moreover, its conductivity declines above 90 °C because anisotropic swelling causes high resistance and poor adhesion between the membrane and electrodes [5].

Several methods have been followed to improve the performance of Nafion membranes and the composite approach has demonstrated to be effective in improving relevant properties of

* Corresponding author. Department of Chemical Science and Technologies & NAST Center, University of Rome Tor Vergata, Via della Ricerca Scientifica, 00133 Rome, Italy. Tel.: +39 (0)6 7259 4389; fax: +39 (0)6 7259 4328.
E-mail address: alessandra.d.epifanio@uniroma2.it (A. D'Epifanio).

0378-7753/$ – see front matter © 2013 Elsevier B.V. All rights reserved.
http://dx.doi.org/10.1016/j.jpowsour.2013.10.070

the electrolyte, since it offers the opportunity to combine the properties of two components, the organic matrix and the inorganic filler, into a unique material [6–8]. Indeed, it was demonstrated that the addition of hygroscopic metal oxides, such as titania, silica, zirconia, in the form of nano- or submicrometric particles improves the cell performance, in terms of higher operating temperature, easier water management, and thermomechanical stability [9]. These results have been attributed to the influence of surface properties of the inorganic filler on the water retention characteristics of the composite and/or to morphological modifications induced by the filler on Nafion [10–12]. Nevertheless, the composite approach not always leads to the desired improvement in fuel cell performance, because non-proton-conductive inorganic species often lower the overall proton conductivity of the composite membrane, in addition to the difficulties in obtaining a uniform dispersion of the ceramic oxide particles in the polymeric matrix [13].

To minimize the proton conductivity losses induced by the introduction of inorganics, the use of several acidic fillers has been investigated. The use of sulfonated zirconium phosphonates, heteropolyacids, or sulphated metal oxides in Nafion composite membranes have led to a general enhancement in the fuel cell response, in terms of both power density delivered and ohmic resistance reduction [14].

Another promising type of fillers is organically modified metal oxides, where organic moieties bearing sulfonic acid groups are covalently bound to the oxide surface [15]. By appropriate design of the functional group it is possible not only to modulate the acidity of the filler, but also to introduce further ionic/non-ionic micro-domains which can affect the morphology of the final composite membrane. It is well know, in fact, that the micro- and nanoscopic phase separation of ionic and non-ionic domains strongly affects key electrolyte properties such as proton conductivity and fuel crossover [4]. The binding of different arylene, alkylic or fluoroalkylic chains onto silica surface and clay materials has been reported in the literature [16,17]. Such materials have been largely used for catalytic applications but not much explored as fillers in composite polymer electrolyte membranes [18].

We here report on the synthesis of propylsulfonic-functionalized titania (TiO_2–RSO_3H), a novel compound to be used as filler in Nafion-based composite membranes. Nanostructured titania was chosen as a starting material since membrane performance is strongly influenced by the filler particle size, higher the interface interaction between the dispersed nanoparticles and the polymeric matrix, greater being the influence of filler on the original characteristics of the electrolyte [19–21].

The synthetic procedure consists in the grafting onto the ceramic oxide surface of silylpropyl moieties bearing terminal sulfonic acid groups, a procedure previously used to enhance the acidity of clay minerals [22,23].

The use of TiO_2–RSO_3H, in which protogenic groups are covalently bound on TiO_2 nanoparticles, is expected to increase the proton conductivity of composite membranes avoiding their excessive swelling in DMFC operative conditions. Furthermore, the presence of bifunctional branches, consisting of hydrophobic aliphatic chains with terminal hydrophilic groups, can ease the uniform dispersion of filler due to the enhanced interfacial compatibility with hydrophobic and hydrophilic Nafion domains.

Composite membranes made of Nafion and containing TiO_2–RSO_3H were prepared, characterized, and tested in a DMFC single cell. The filler content was varied from 5 up to 20 wt.% to identify the electrolyte composition with the lowest methanol permeability, the highest proton conductivity and the best dimensional stability with respect to unfilled Nafion membrane.

2. Experimental

2.1. Materials

Titanium (IV) isopropoxide, (3-Mercaptopropyl)trimethoxysilane (95%, MPTMS), N,N-dimethylacetamide (DMAc) and Nafion perfluorinated resin solution (5 wt.% in a mixture of lower aliphatic alcohols and water) were purchased from Sigma–Aldrich and used as received. Hydrogen peroxide (40% m v^{-1} in water) and all solvents were purchased by Carlo Erba and used without further purification.

2.1.1. Synthesis of propylsulfonic-functionalized titania

Nanometric TiO_2 was prepared as previously reported [6]. TiO_2–RSO_3H was prepared as follows: MPTMS (480 μL, 2.58 mmol) was added to a suspension of 1 g of TiO_2 in 10 mL of toluene and the mixture was stirred at 80 °C overnight. The powder was recovered by filtration, washed twice with toluene (10 mL) and dried under vacuum at 60 °C overnight. The product was reacted with H_2O_2 40% m v^{-1} (140 mL) for 6 h at 50 °C under stirring. The reaction product was recovered by filtration and dried under vacuum for 2 h at 60 °C.

El. An.: %C: 0.52; %H: 0.26; %S: 0.18; %Ti: 15.3; %Si: 0.3.

2.1.2. Membranes preparation

Composite membranes with 5, 10 and 20 wt.% TiO_2–RSO_3H content (N_5TiO_2–RSO_3H, N_10TiO_2–RSO_3H and N_20TiO_2–RSO_3H, respectively) were prepared as follows. Nafion solution (12 mL) was added to DMAc. The solution was heated to 80 °C to evaporate low-boiling solvents. During the evaporation step DMAc was added to maintain the solution volume around 15 mL. This process was repeated three times to ensure that the original solvent was replaced by DMAc. The TiO_2–RSO_3H powder was dispersed in DMAc and the resulting suspension was kept under stirring for 4 h at RT, then added to the Nafion solution. The suspension was then casted in a Petri dish and dried at 80 °C overnight. Composites containing 5 wt.% of TiO_2 (N_5TiO_2) and unfilled Nafion membranes (N_RC) were also prepared and used as references. The thickness of the membranes ranged between 80 and 130 μm. The membranes selected for polarization and methanol permeability tests had a thickness of 100 μm (±5%). Before characterization, all the membranes were treated in a standard activation procedure using H_2O_2 3 vol.% solution, 0.5 M H_2SO_4 solution and distilled water, boiling the samples for 1 h in each solution [14].

2.2. Methods

2.2.1. Characterization of propylsulfonic-functionalized titania

The determination of C, H and S content in the samples was performed using the dynamic flash combustion method: combustion of material followed by gas chromatography determination (CHNS/O analyzer-EAS1108, Fisons instruments). Ti and Si contents in the samples were determined by Neutron Activation Analysis (NAA) using a Slowpoke nuclear reactor, atomic energy of Canada limited pneumatic transfer system; germanium semiconductor gamma-ray detector (Ortec model GEM55185); multichannel analyzer (Ortec model DSPEC Pro) and balance (Mettler Toledo model AT200).

FT–IR spectra were acquired by means of a Perkin–Elmer Spectrum 100 spectrophotometer (16 scans at a resolution of 4 cm^{-1}). The powders were pelleted with KBr and analyzed in transmission mode. Thermal analysis TG/DTA were carried out in the 25–1000 °C temperature range, using a thermobalance 207 (STA 409, Netzsch), in air flow (80 mL min^{-1}) with a heating rate of 2 °C min^{-1}.

Ion exchange capacity (IEC) and water uptake (WU) were measured by typical experiments previously reported [8,12]

2.2.2. Conductivity

Through-plane proton conductivity was measured by electrochemical impedance spectroscopy (EIS) using a multichannel potentiostat (VMP3 BioLogic Science Instruments). An applied voltage of 25 mV and a frequency range of 1 MHz–1 Hz were used. Membrane disks of 8 mm in diameter and powders in the shape of pellets of 13 mm diameter were sandwiched between gas diffusion electrodes (E-Tek ELAT HT 140E-W with a Pt loading of 5 mg cm^{-2}). In the case of membranes/electrode systems a constant torque of 5.0 N m was applied. The measurements were performed as a function of temperature at saturated water vapor pressure (100% RH). Before measurements, the samples were equilibrated overnight at room temperature and saturated humidity. The resistance of the samples, and hence their conductivity, was calculated by fitting the impedance spectra in their linear portion.

2.2.3. DMFC tests, in-situ EIS, and methanol permeation measurements

Membrane electrode assemblies (MEAs) were prepared sandwiching the electrolyte membranes between the anode and cathode by hot pressing at 120 °C under 3.75 MPa for 7 min. Commercial Etek electrodes were used as anode and cathode, respectively: ELAT GDE V 2.2T Single Sided Coating, custom 3 mg cm^{-2} TM loading using 60%Pt:Ru (1:1 a/o) on Vulcan XC-72 and custom 0.8 mg cm^{-2} Nafion application, and ELAT(R) GDE microporous layer including 5 g m^{-2}Pt electrode on woven web. DMFC performance was evaluated by placing the MEAs in a single cell (Fuel Cell Technologies, Inc.) with active area of 5 cm^2. Cells were sealed at a constant torque of 6 N m. A home-made test station was used, feeding the anode with a 2 M methanol solution and the cathode with humidified oxygen. The feeding supply of methanol was monitored by a KNF's Model FEM 1.08 Liquid Metering Pump with control board (flow rate: 2.5 mL min^{-1}, pressure: 2 abs bar). The oxygen supply was controlled by a MKS PR4000 mass-flow controller (flow rate: 150 sccm, pressure: 2 abs bar), and the humidifier temperature was opportunely set to ensure 100% RH of the gas [24]. Polarization and power density (PD) curves were obtained using a Multichannel Potentiostat (VMP3 BioLogic Science Instruments) in the temperature range between 70 and 110 °C.

In situ EIS measurements were performed during the cell operation and in the potentiostatic mode between 0.2 and 0.6 V. An AC sinusoidal perturbation (amplitude 25 mV) was introduced to the DC load, and impedance spectra were acquired by sweeping frequencies over the 50 KHz–100 mHz.

Methanol permeation was evaluated after polarizations test according to a voltametric method previously reported [14,25]. (anode feed: 2 M methanol solution at a flow rate of 2.5 mL min^{-1}; cathode feed: humidified N_2). The limiting current density (J_{lim}) was measured at 80 °C, applying a voltage from 0 to 0.9 V (scan rate: 2 mV s^{-1}). Membrane selectivity (α) was calculated as the ratio of proton conductivity to methanol permeability [26].

3. Results and discussion

Titania powder was synthesized *via* sol–gel reaction from the relative alkoxide and calcined at 450 °C to obtain the nanostructured oxide which lends itself well to further functionalization, due to the presence of an adequate amount of surface hydroxyl groups, and is, at the same time, insoluble and thermally stable in DMFCs operative conditions [24,27].

The surface functionalization of TiO_2 particles was carried out using MPTMS as grafting agent. The procedure has been largely and successfully used to introduce thiolic functionalities onto silica surface [28,29], but scarcely investigated for other metal oxides.

The synthesis was carried out following the synthetic pathway shown in Fig. 1: *i*) silylation of the surface hydroxyl groups with MPTMS to obtain mercaptopropyl-modified titania (TiO_2–RSH); *ii*) subsequent oxidation of the thiol groups into sulfonic acid groups to obtain propylsulfonic-functionalized titania (TiO_2–RSO_3H).

Fig. 2 shows the FT–IR spectra of TiO_2 and TiO_2–RSO_3H. Both spectra show a broad absorption centered at 600 cm^{-1}, in the region where the lattice Ti–O stretching band appears, while the broad absorption between 3700 and 3000 cm^{-1} and a sharper peak at 1640 cm^{-1} are due to the stretching vibrations of the hydroxyl groups on the surface of titania nanoparticles and physisorbed water [30]. Grafting of Si-propylsulphonic groups on the oxide surface is demonstrated by the presence in the spectrum of TiO_2–RSO_3H of a band centered at 1000 cm^{-1} assigned to the Si–O stretching vibrations [22,28,29]. Moreover, the propyl groups are identified by the methylene stretching bands in the 2950–2850 cm^{-1} region, and by the methylene bending bands in the 1450–1200 cm^{-1} region (in overlap with the asymmetric stretching band of the SO_3H moieties at 1350 cm^{-1}).

The amount of (–RSO_3H) was quantified by NAA and CHS analyses. The content of functional groups was estimated to be 0.12 mmol g^{-1}, corresponding to 2 wt.%.

The presence of sulfur and silicon in the propylsulfonic-functionalized titania was also verified *via* EDX microanalysis. Sulfur and silicon peaks were clearly visible in the EDX spectrum of TiO_2–RSO_3H (not shown).

TG/DTA was carried out to study the thermal stability of TiO_2–RSO_3H and to evaluate its applicability in the DMFC operating temperature range. Fig. 3 shows the thermogravimetric–differential thermogravimetric analysis TG–DTA curves of TiO_2–RSO_3H compared with those of pristine TiO_2. The TG/DTA curves for calcined titania show as single feature a broad endothermic peak centered at 100 °C, associated with a 2% weight loss of physisorbed water [31]. The introduction of the highly hygroscopic sulfonic acid groups results in a two-steps water loss extended over a wider temperature range: the first endothermic peak (ca. 125 °C, 3% weight loss) is due to the desorption of physisorbed water, the second one (ca. 220 °C, 1% weight loss) can be attributed to more strongly bound water molecules. Finally, the broad exothermic peak centered at 378 °C is assigned to the decomposition of propylsulfonic groups [15,29].

The success of the preparative procedure was also confirmed by the comparison of the ion exchange capacity value of TiO_2–RSO_3H (0.46 meq g^{-1}) with the value measured for TiO_2 (0.12 meq g^{-1}).

Fig. 4 shows the Arrhenius plots for the two oxides in the 20–140 °C range, at RH 100%. The conductivity of TiO_2–RSO_3H was almost one order of magnitude higher in the whole investigated temperature range (3.5 10^{-3} S cm^{-1} for TiO_2–RSO_3H *vs.* 4.17 10^{-4} S cm^{-1} for TiO_2 at 140 °C). The addition of –RSO_3H groups on the oxide surface favors proton transport also at a high temperature providing new acidic sites, in agreement with TG/DTA results which showed the higher thermal stability of the hydration shell of the sulfonic acid groups.

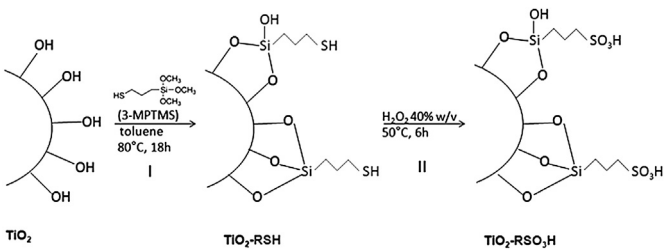

Fig. 1. Synthetic pathway for the surface functionalization of TiO_2 nanoparticles.

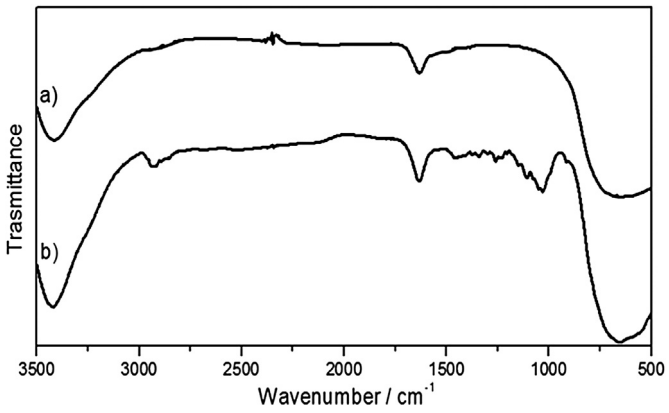

Fig. 2. FTIR spectra of TiO_2(a) and TiO_2–RSO_3H(b).

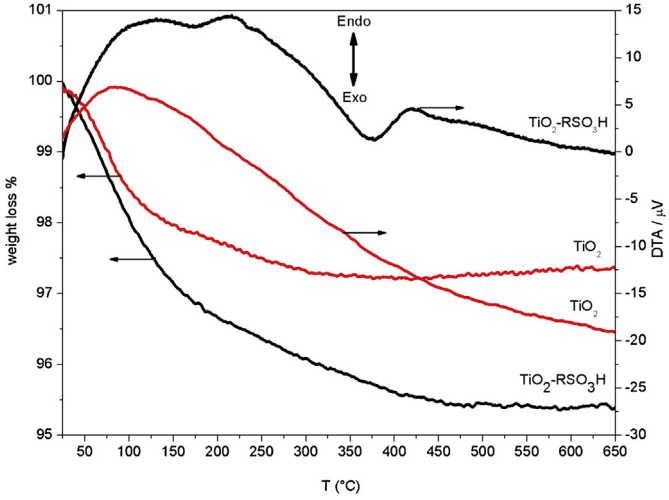

Fig. 3. TG/DTA curves of TiO_2 and TiO_2–RSO_3H.

All the characterization data converge to indicate the success of the propylsulfonic functionalization of titania and its potential applicability in the temperature range of exercise of a DMFC.

Unfilled and composite Nafion membranes with various filler content were prepared by solution casting from DMAc. The water uptake (WU) at room temperature RT of the nanocomposite membranes decreased as a function of TiO_2–RSO_3H content ranging from 32 wt % for reference Nafion to 12 wt % for the composite containing 20 wt.% TiO_2–RSO_3H. The observed reduction of WU due to the incorporation of the hybrid oxide into the Nafion matrix might avoid failure in mechanical properties reducing the membrane free volume and swelling characteristics.

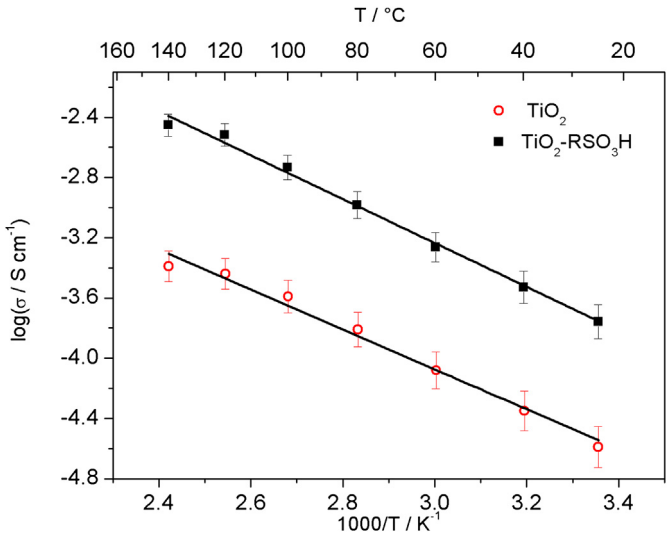

Fig. 4. Arrhenius plots of TiO_2 and TiO_2–RSO_3H, at RH 100%.

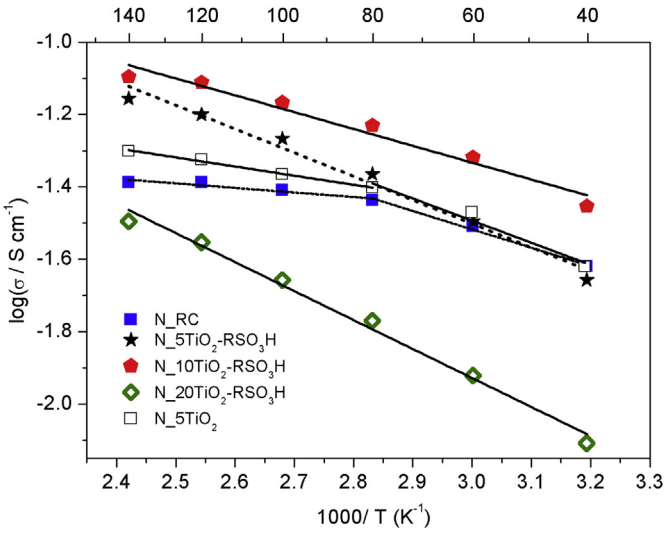

Fig. 5. Arrhenius plot of unfilled and composite Nafion membranes, at RH = 100%.

The effect of the TiO_2 and TiO_2–RSO_3H content on conductivity was investigated and the resulting Arrhenius plots (RH = 100%) are shown in Fig. 5. It is evident that the use of the functionalized filler is to be preferred as it increased the proton conductivity of the electrolyte membrane in the whole investigated temperature range as shown by the comparison of data relative to N_5TiO_2SO_3H and N_5TiO_2. The composite membranes conductivity increased with increasing filler content up to 10 wt.% (σ = 0.08 Scm^{-1} at 140 °C), then a marked decrease was observed for the sample with 20 wt.% of filler which conductivity was lower than that of reference Nafion.

This trend suggests that an excessive amount of metal oxide nanoparticles occludes the hydrophilic clusters of the membrane blocking proton transfer [32]. The reference Nafion membrane showed two different proton conductivity regions. σ values

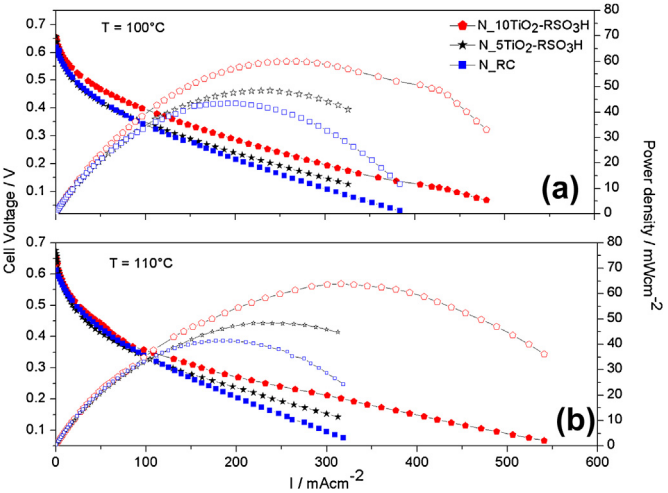

Fig. 6. Polarization and PD curves of unfilled Nafion and composite membranes at 100 (a) and 110 °C (b).

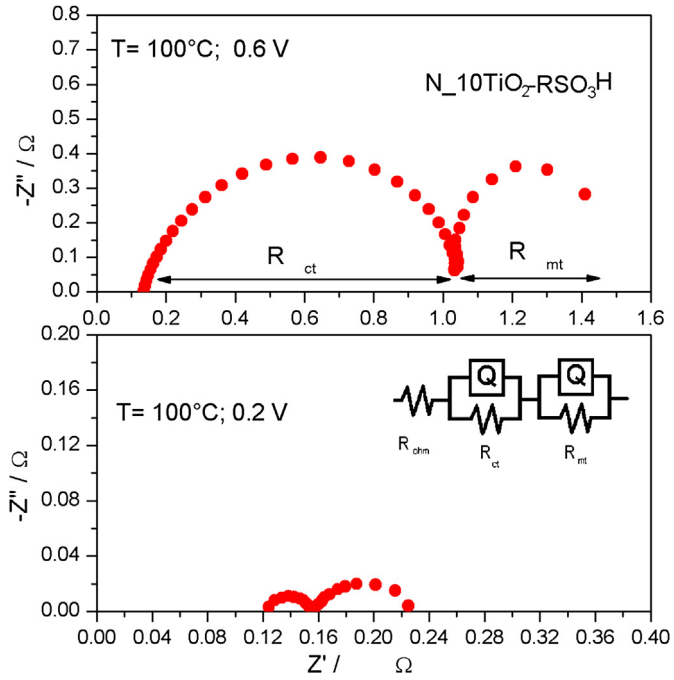

Fig. 7. Typical Nyquist plot of MEA made up with N_10TiO_2–RSO_3H composite membrane, collected at 0.2 V and 0.6 V at 100 °C.

increased with increasing temperature in the first region (40–80 °C), while remained almost constant in the last one (80–140 °C). The structural changes occurring in the water swollen membrane lead to bulk-like proton conductivity at high hydration levels, with a subsequent decrease in activation energy [33]. On the contrary, composite membranes showed the same trend in the whole range of investigated temperatures, confirming their lower tendency to swell with respect to unfilled Nafion membrane. Thus, although there is a threshold value of filler content to improve the performance of the composites, it is noteworthy that the loading of appropriate amount of propylsulfonic-functionalized titania allows to obtain Nafion-based composite membranes with higher conductivity values and dimensional stability up to 140 °C.

To check the applicability of the Nafion-based composite membranes in a real device, the electrochemical performance of the electrolytes was tested in a DMFC single cell. Fig. 6a and b shows polarization (I–V) and power density (PD) curves for the unfilled Nafion and composite membranes at 100 and 110 °C. At both temperatures, composite membranes showed higher performance than Nafion. N_RC membrane showed a decline of performance with the increasing of temperature at 110 °C (PD_{max} = 40 mW cm^{-2} and $I_{(0.2\ V)}$ = 202 mA cm^{-2}), in agreement with its well-known loss in stability above 90 °C. On the contrary, the N_5TiO_2–RSO_3H membrane maintained almost the same PD and I values with respect to those recorded at 100 °C (PD_{max} = 48 mW cm^{-2} and $I_{(0.2\ V)}$ = 240 mA cm^{-2}). The best performance was determined for N_10TiO_2–RSO_3H at 110 °C (PD_{max} = 64 mW cm^{-2} and $I_{(0.2\ V)}$ = 316 mA cm^{-2}), with a PD improvement about of 40% with respect to N_RC membrane at the same temperature.

The impedance characteristics of the DMFC under different operating temperatures (70–110 °C) were also investigated. Fig. 7 shows a typical Nyquist plot of MEA made up with N_10TiO_2–RSO_3H composite membrane, collected at 0.2 V and 0.6 V at 100 °C. All the spectra showed one arc at high frequencies accounting for the charge transfer resistance (R_{ct}), prevailing at 0.6 V, and one arc at low frequencies accounting for mass transfer processes (R_{mass}), prevailing at 0.2 V [34,35]. Fig. 8 shows the variation of R_{ct} and R_{mass} for three MEAs equipped with N_RC, N_5TiO_2–RSO_3H and N_10TiO_2–RSO_3H as a function of temperature, at 0.6 V and at 0.2 V. Both R_{ct} and R_{mass} values are lower for the MEAs with the composite membranes in the whole range of investigated temperatures and particularly at higher temperatures, where the MEA with N_10TiO_2–RSO_3H shows the lowest resistances. The decrease of R_{ct} and R_{mass} observed for the composites can be attributed to improved membrane/electrode interface stability, being all MEA components identical, except for the membranes.

To correlate the observed improved performance with methanol permeability, steady-state limiting methanol oxidation current density (J_{lim}) value through the unfilled Nafion was measured and compared with that of N_10TiO_2–RSO_3H, that is the composite membrane with the best performance in terms of proton conductivity and PD delivered in DMFC tests. Fig. 9 shows the voltammetric curves resulting from electro-oxidation of methanol permeating through the membranes at 80 °C, J_{lim} value corresponding to the current densities plateau. The microstructural changes induced by the presence of the functionalized filler result in an 18% decrease of J_{lim} for sample N_10TiO_2–RSO_3H with respect to reference Nafion [4]. The methanol permeability values for N_RC and N_10TiO_2–RSO_3H were calculated according to a previously

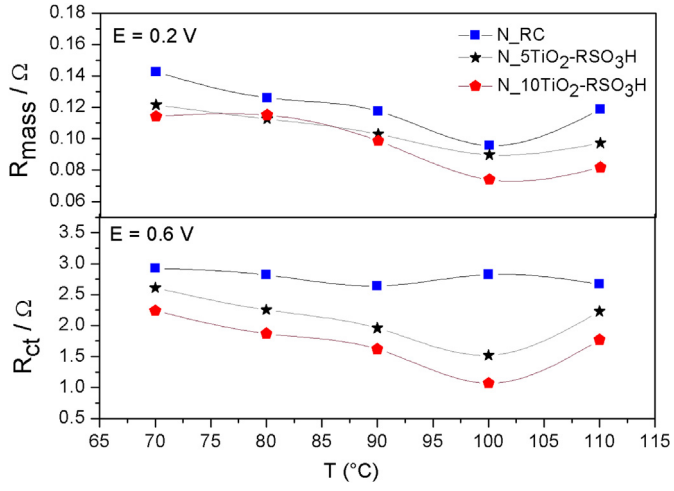

Fig. 8. R_{ct} and R_{mass} as a function of temperature for unfilled Nafion and composite membranes.

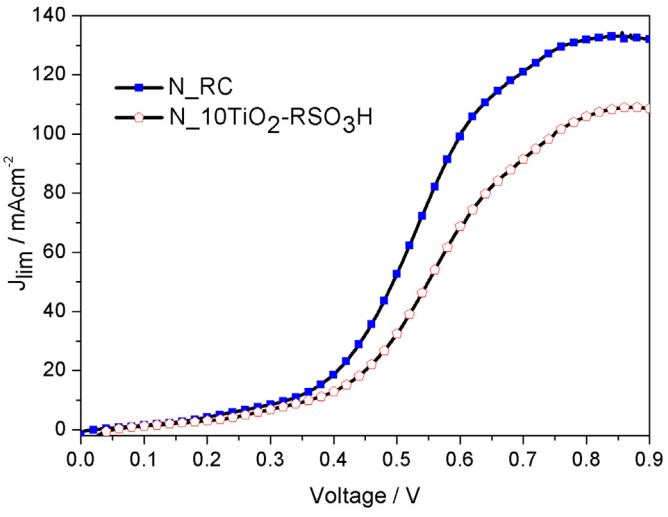

Fig. 9. Voltammetric curve for the oxidation of methanol permeating through unfilled Nafion and N_10TiO_2–RSO_3H composite membrane T = 80 °C.

Table 1
Methanol permeability and membrane selectivity of N_RC and N_10TiO_2–RSO_3H at 80 °C.

	Methanol permeability × 10^{-7} (DH_{LC}/cm^2 s^{-1})	Selectivity × 10^{-4} (α/S scm^{-3})
N_RC	1.05	3.98
N_10TiO_2–RSO_3H	0.75	7.8

reported method [25], while selectivity of membranes was evaluated as the ratio between proton conductivity and methanol permeability [26]. As anticipated from conductivity and permeability measurements, the N_10TiO_2–RSO_3H membrane showed enhanced selectivity with respect to unfilled Nafion membrane (Table 1).

These results suggest that the improvement of the composite membranes performance in DMFC can be ascribed to both the higher conductivity values and lower methanol permeability.

4. Conclusions

A simple surface functionalization method was successfully used onto titania nanoparticles, which were decorated with propylsulfonic acid groups (TiO_2–RSO_3H). The grafting of propylsulfonic-groups on the titania surface was confirmed by FT–IR spectroscopy, TG/DTA and elemental analysis.

The introduction of covalently bound sulfonic acid groups led to increased IEC and improved the capacity of the material to retain more and more strongly bound water. Furthermore, TiO_2–RSO_3H resulted to be thermally stable in the DMFC operative temperature range. As a consequence, the proton conductivity values of TiO_2–RSO_3H resulted to be higher than those of TiO_2 in a wide range of temperature, reaching $3.5 \cdot 10^{-3}$ Scm^{-1} at 140 °C.

Composite membranes were prepared embedding TiO_2–RSO_3H into Nafion matrix. They showed lower WU and superior conductivity compared to unfilled Nafion membrane. In particular, N_10TiO_2–RSO_3H membrane showed the highest proton conductivity reaching 0.08 S cm^{-1} at 140 °C. The MEA assembled using such composite as electrolyte showed lower methanol permeability, higher selectivity ratio and a PD improvement of about 40% with respect to that obtained with Nafion membrane in DMFC tests at 110 °C. These results qualify the propylsulfonic-functionalized titania as a valid proton-conducting filler to be used in Nafion-based composite membranes operating at temperatures higher than 100 °C.

Acknowledgments

The authors thank Ms C. D'Ottavi for her valuable technical support.

The financial support of the Italian Ministry for University and Research under the framework of the PRIN 2010-11 project "Advanced nanocomposite membranes and innovative electro catalysts for durable polymer electrolyte membrane fuel cells, NAMED-PEM" and Ministère du Développement économique, de l'Innovation et de l'Exportation (Quebec, Canada) are gratefully acknowledged.

References

[1] A.S. Aricò, S. Srinivasan, V. Antonucci, Fuel Cells 1 (2001) 133–161.
[2] V. Baglio, A. Di Blasi, A.S. Aricò, V. Antonucci, P.L. Antonucci, C. Trakanprapai, V. Esposito, S. Licoccia, E. Traversa, J. Electrochem. Soc. 152 (2005) A1373–A1377.
[3] T.A. Zawodzinski, M. Neeman, L.O. Sillerud, S. Gottesfeld, J. Phys. Chem. 95 (1991) 6040–6044.
[4] K.D. Kreuer, J. Membr. Sci. 185 (2001) 29–39.
[5] M. Casciola, G. Alberti, M. Sganappa, R. Narducci, J. Power Sources 162 (2006) 141–145.
[6] S. Licoccia, E. Traversa, J. Power Sources 159 (2006) 12–20.
[7] A. Saccà, A. Carbone, E. Passalacqua, A. D'Epifanio, S. Licoccia, E. Traversa, E. Sala, F. Traini, R. Ornelas, J. Power Sources 152 (2005) 16–21.
[8] B. Mecheri, V. Felice, Z. Zhang, A. D'Epifanio, S. Licoccia, A.C. Tavares, J. Phys. Chem. C 116 (2012) 20820–20829.
[9] S. Bose, T. Kuila, T.X.H. Nguyen, N.H. Kim, K. Lau, J.H. Lee, Prog. Polym. Sci. 36 (2011) 813–843.
[10] N.H. Jalani, K. Dunn, R. Datta, Electrochim. Acta 51 (2005) 553–560.
[11] O. Savadogo, J. Power Sources 127 (2004) 135–161.
[12] A. D'Epifanio, M.A. Navarra, F.C. Weise, B. Mecheri, J. Farrington, S. Licoccia, S. Greenbaum, Chem. Mater. 22 (2010) 813–821.
[13] D.H. Jung, S.Y. Cho, D.H. Peck, D.R. Shin, J.S. Kim, J. Power Sources 106 (2002) 173–177.
[14] F. Chen, B. Mecheri, A. D'Epifanio, E. Traversa, S. Licoccia, Fuel Cells 10 (2010) 790–797.
[15] C.H. Rhee, Y. Kim, J.S. Lee, H.K. Kim, H. Chang, J. Power Sources 159 (2006) 1015–1024.
[16] J.A. Melero, R. vanGrieken, G. Morales, Chem. Rev. 106 (2006) 3790–3812.
[17] C.H. Rhee, H.K. Kim, H. Chang, J.S. Lee, Chem. Mater. 17 (2005) 1691–1697.
[18] A. Corma, H. Garcia, Adv. Synth. Catal. 348 (2006) 1391–1412.
[19] G. Alberti, M. Casciola, Annu. Rev. Mater. Res. 33 (2003) 129–154.
[20] C. de Bonis, A. D'Epifanio, B. Mecheri, E. Traversa, M. Miyayama, A.C. Tavares, S. Licoccia, Solid State Ionics 227 (2012) 73–79.
[21] D. Marani, A. D'Epifanio, E. Traversa, M. Miyayama, S. Licoccia, Chem. Mater. 22 (2010) 1126–1133.
[22] C.S. Gill, B.A. Price, C.W. Jones, J. Catal. 251 (2007) 145–152.
[23] V. Felice, S. Ntais, A.C. Tavares, Microporous Mesoporous Mater. 169 (2013) 128–136.
[24] A. D'Epifanio, B. Mecheri, E. Fabbri, A. Rainer, E. Traversa, S. Licoccia, J. Electrochem. Soc. 154 (2007) B1148–B1151.
[25] X. Ren, T.E. Springer, T.A. Zawodzinski, S. Gottesfeld, J. Electrochem.Soc. 147 (2000) 466–474.
[26] Y.A. Elabd, E. Napadensky, J.M. Sloan, D.M. Crawford, C.W. Walker, J. Membr. Sci. 217 (2003) 227–242.
[27] R. O'Hayre, S.-W. Cha, W. Colella, F.B. Prinz, Fuel Cell Fundamentals, John Wiley & Sons, New York, NY, 2006.
[28] S. Shylesh, S. Sharma, S.P. Mirajkar, A.P. Singh, J. Mol. Catal. A Chem. 212 (2004) 219–228.
[29] D. Margolese, J.A. Melero, S.C. Christiansen, B.F. Chmelka, G.D. Stucky, Chem. Mater. 12 (2000) 2448–2459.
[30] P.A. Connor, K.D. Dobson, A.J. McQuillan, Langmuir 15 (1999) 2402–2408.
[31] K. Porkodi, S. Daisy Arokiamary, Mater. Charact. 58 (2007) 495–503.
[32] C.Y. Yen, C.H. Lee, Y.F. Lin, H.L. Lin, Y.H. Hsiao, S.H. Liao, C.Y. Chuang, C.C.M. Ma, J. Power Sources 173 (2007) 36–44.
[33] M. Eikerling, A.A. Kornyshev, J. Electroanal. Chem. 502 (2001) 1–14.
[34] X. Yuan, H. Wang, J.C. Sun, J. Zhang, Int. J. Hydrogen Energy 32 (2007) 4365–4380.
[35] J.T. Mueller, P.M. Urban, J. Power Sources 75 (1998) 139–143.